Sum Rules for Magnetic Dichroism in Rare Earth 4*f* Photoemission

B. T. Thole[1] and G. van der Laan[2]

[1]*Materials Science Center, University of Groningen, 9747 AG Groningen, The Netherlands*
[2]*Daresbury Laboratory, Warrington WA4 4AD, United Kingdom*

(Received 12 November 1992)

We present new sum rules for magnetic dichroism in spin polarized photoemission from partly filled shells which give the expectation values of the orbital and spin magnetic moments and their correlations in the ground state. We apply this to the 4*f* photoemission of rare earths, where the polarization effects are 2 orders of magnitude larger than in 3*d* transition metals. The very strong dichroism in the 4*f* electron yield opens new perspectives for the characterization of magnetic rare earth surfaces and thin films.

PACS numbers: 79.60.−i, 78.20.Ls, 75.50.Cc

Magnetic circular and linear dichroism in core level spectroscopy is rapidly developing as a tool to obtain valuable information about the electronic and magnetic structure of solids, thin films, and multilayers [1]. In the core level photoemission the magnetic circular dichroism has been analyzed in terms of the alignment between the valence spin and the core hole orbital momentum [2]. Although this provides large effects in the individual peaks, such as in the Fe 2*p* photoemission of ferromagnetic iron [3], the integrated magnetic circular dichroism is zero because there is no net preference for left or right polarization in the dipole transition from a completely filled core level to an empty continuum state. The situation is different for emission from a partly filled (open) shell with spin and orbital momentum, where a nonstatistical distribution of the population over the orbital magnetic sublevels results in a difference in the integrated photoemission for left ($\Delta M=-1$) and right ($\Delta M=+1$) circularly polarized radiation. Similarly, a nonstatistical distribution over the spin states gives different integrated photoemission intensities for spin up and spin down. Thus the integrated photoemission (or partial electron yield) from an open shell contains information about the spin and orbital momenta in the initial state. In this Letter we derive general sum rules which show that specific linear combinations of the light and spin polarized spectra have integrated intensities that are proportional to the ground state expectation values of spin and orbital momentum products. These results make it possible to use polarized photoemission as a simple analytical tool which is of great importance to experimentalists. As an illustration we analyze two theoretical examples of 4*f* photoemission. The dichroism in the 4*f* electron yield is so large that it promises interesting technological applications for the study of magnetic domain structures of surfaces, thin films, and multilayers.

First we give a theoretical derivation of the photoemission sum rules which are valid under quite general circumstances. The main restrictions are that we allow only one final state channel, and a constant radial matrix element for electron excitation to the continuum. For photoemission far above the continuum onset the $\Delta l=+1$ channel dominates and the photoelectron is insensitive to the details of the lattice potential; thus the error of these approximations is small. However, experimentally it is often difficult to separate the contributions from the different l shells. An exception to this is the 4*f* photoemission of the rare earths, which has a much larger cross section and is at higher binding energy than the other valence states [4]. Due to the corelike character of the 4*f* the photoemission spectrum can be explained completely by atomic multiplet theory as has been shown for the isotropic spectra by Lang, Baer, and Cox [5] and Gerken [6] and for the magnetic circular dichroism by the recent experimental results of Starke *et al.* [7].

The dipole matrix element for transition from a ground state $\langle\psi|$ to a final state $|\psi'\rangle$ creating a free electron with orbital momentum m' and spin σ in a continuum shell c is

$$D_{m'\sigma}=\sum_m \langle\psi|l^\dagger_{m\sigma}c_{m'\sigma}|\psi'\rangle\langle lm|rC^{(1)}_q|cm'\rangle\,, \tag{1}$$

where $C^{(1)}_q$ is a normalized spherical harmonic; $q=-1,0,+1$ denotes right circularly, z, and left circularly polarized radiation, respectively; and $l^\dagger_{m\sigma}$ and $c_{m'\sigma}$ denote the creation and annihilation operator for an l shell and c continuum electron, respectively. $\langle\psi|$ can be any state containing electrons in a shell with angular momentum l, such as a mixture of l^n, $l^{n+1}\underline{v}$, $l^{n+2}\underline{v}^2$, where $\underline{v}$ denotes a hole in any shell that has no dipole matrix element with the continuum shell $c=l\pm1$. Thus the following treatment includes the presence of Coulomb and spin-orbit interactions and of crystal and exchange fields of any symmetry. It is assumed that ψ has no continuum electrons in c.

The integrated intensity of the angle integrated spectrum for a fixed value of σ is obtained by summing over all ψ' and m'

$$\rho_{q\sigma}=\sum_{\psi'}\sum_{m\underline{m}}\langle\psi|l^\dagger_{m\sigma}c_{m'\sigma}|\psi'\rangle\langle\psi'|c^\dagger_{m'\sigma}l_{\underline{m}\sigma}|\psi\rangle \times\langle lm|rC^{(1)}_q|cm'\rangle\langle cm'|rC^{(1)}_{-q}|l\underline{m}\rangle\,. \tag{2}$$

We sum over ψ' using the closure relation. Further, because of the selection rules on the one-electron matrix elements, we have $m=\underline{m}$, which gives the following interpretation its simplicity:

$$\rho_{q\sigma}=\sum_m\langle\psi|l^\dagger_{m\sigma}l_{m\sigma}|\psi\rangle\sum_{m'}|\langle lm|rC^{(1)}_q|lm'\rangle|^2$$
$$\propto\sum_m\langle n_{m\sigma}\rangle\begin{pmatrix} l & 1 & c\\ -m & q & -q+m\end{pmatrix}^2. \quad (3)$$

Thus the integrated intensity $\rho_{q\sigma}$ is simply the sum over each $m\sigma$ sublevel of its occupation number times the total transition probability of that sublevel to the c shell. We have used the Wigner-Eckart theorem and omitted the radial matrix element because we discuss only relative intensities.

Using a recoupling, we found that the squared 3-j symbol can be written in a very powerful way that directly allows us to separate the operators measured using different light polarizations,

$$\rho_{q\sigma}=\sum_m\langle n_{m\sigma}\rangle\{\tfrac{1}{3}A_0+\tfrac{1}{2}A_1qm+\tfrac{1}{2}A_2(q^2-\tfrac{2}{3})[m^2-\tfrac{1}{3}l(l+1)]\}, \quad (4)$$

where

$$A_0=\frac{1}{2l+1}, \quad (5)$$

$$A_1=\frac{l(l+1)+2-c(c+1)}{l(2l+1)(2l+2)}, \quad (6)$$

$$A_2=\frac{6[3K(K-1)-8l(l+1)]}{(2l-1)(2l)(2l+1)(2l+2)(2l+3)}, \quad (7)$$
$$K=l(l+1)+2-c(c+1).$$

It can be easily checked that expectation values of various powers $m^x\sigma^y$ can be obtained by selecting the appropriate term from Eq. (4). This can be done by taking the linear combinations ρ^{xy} of the $\rho_{q\sigma}$ which are given in Eqs. (8)–(13), where the superscript $x=0,1,2$ denotes the isotropic spectrum and the circular and linear dichroism, respectively, and $y=0,1$ denotes without and with spin polarization, respectively.

First of all, for the integrated isotropic spectrum we find

$$\rho^{00}\equiv\rho_{1\uparrow}+\rho_{0\uparrow}+\rho_{-1\uparrow}+\rho_{1\downarrow}+\rho_{0\downarrow}+\rho_{-1\downarrow}$$
$$=A_0\sum_{m\sigma}\langle n_{m\sigma}\rangle=A_0\langle n\rangle, \quad (8)$$

where $\uparrow$ and $\downarrow$ mean $\sigma=\pm\frac{1}{2}$. Thus ρ^{00} measures the number of electrons in the l shell.

Likewise, we find for the integrated spin spectrum, introducing a factor $2\sigma=\pm1$ to multiply the spin-down spectra,

$$\rho^{01}\equiv\rho_{1\uparrow}+\rho_{0\uparrow}+\rho_{-1\uparrow}-\rho_{1\downarrow}-\rho_{0\downarrow}-\rho_{-1\downarrow}$$
$$=2A_0\sum_{m\sigma}\langle n_{m\sigma}\rangle\sigma=2A_0\langle S_{z'}\rangle, \quad (9)$$

which measures the spin magnetic moment.

For the integrated circular dichroism we obtain

$$\rho^{10}\equiv\rho_{1\uparrow}-\rho_{-1\uparrow}+\rho_{1\downarrow}-\rho_{-1\downarrow}=A_1\sum_{m\sigma}\langle n_{m\sigma}\rangle m=A_1\langle L_z\rangle, \quad (10)$$

giving the orbital magnetic moment just as in x-ray absorption [8], which is a particle-hole analog of valence photoemission replacing the continuum shell by a core level.

For the integrated spin-orbit spectrum we obtain

$$\rho^{11}\equiv\rho_{1\uparrow}-\rho_{-1\uparrow}-\rho_{1\downarrow}+\rho_{-1\downarrow}$$
$$=2A_1\sum_{m\sigma}\langle n_{m\sigma}\rangle m\sigma=2A_1\left\langle\sum_i l_z(i)s_{z'}(i)\right\rangle, \quad (11)$$

where l_z and $s_{z'}$ are defined as one-electron operators acting only on l-shell functions, contrary to L and S which are sums of these over all electrons, and measure only properties of l-shell electrons. Thus ρ^{11} gives the correlation of the z component of l and the z' component of s. For this effect no magnetic polarization is needed. For example, for isotropic ions and $z=z'$ it is simply one-third of the spin-orbit coupling. When there is magnetic polarization it measures the amount in which l_z is polarized by $s_{z'}$ due to spin-orbit coupling.

For the integrated linear dichroism we obtain

$$\rho^{20}\equiv\rho_{1\uparrow}-2\rho_{0\uparrow}+\rho_{-1\uparrow}+\rho_{1\downarrow}-2\rho_{0\downarrow}+\rho_{-1\downarrow}$$
$$=A_2\sum_{m\sigma}\langle n_{m\sigma}\rangle[m^2-\tfrac{1}{3}l(l+1)]=A_2\langle Q_{zz}\rangle, \quad (12)$$

which measures the quadrupole moment Q_{zz} of the ion. A positive value means that high values of $|m|$ are occupied which makes the ion flat in the x-y plane. For a negative value it is elongated along the z axis. This quantity is nonzero not only in ferromagnets and antiferromagnets, but also in spatially anisotropic media even if nonmagnetic (crystal fields).

For the anisotropy of the spin distribution we find

$$\rho^{21}\equiv\rho_{1\uparrow}-2\rho_{0\uparrow}+\rho_{-1\uparrow}-\rho_{1\downarrow}+2\rho_{0\downarrow}-\rho_{-1\downarrow}$$
$$=2A_2\sum_{m\sigma}\langle n_{m\sigma}\rangle[m^2-\tfrac{1}{3}l(l+1)]\sigma$$
$$=2A_2\left\langle\sum_i q_{zz}(i)s_{z'}(i)\right\rangle, \quad (13)$$

where q_{zz} is defined as the one-electron operator $l_z^2-\frac{1}{3}l(l+1)$. Like ρ^{11} it has a value if both $S_{z'}$ and Q_{zz} are nonisotropic, but when S is unpolarized there is still a contribution if spin-orbit coupling gives the spin a different value when the electron is along the z axis or in the x-y plane.

In order to show the magnitude of the polarization effects we present the theoretical photoemission signals I^{xy} (the fundamental spectra) which are defined as the six combinations of the primitive spectra $I_{q\sigma}$ in Eqs. (8)–(13). Because the symmetries of configurations with less and more than half-filled f shells are different, we give examples for Nd^{3+} $4f^3$ in Fig. 1 and Ho^{3+} $4f^{10}$ in Fig. 2. The photoemission from their Hund's rule ground states with $M=-J$ to the εg continuum was calculated in intermediate coupling using Cowan's code [9]. The integrated intensities of the fundamental spectra are given in Table I.

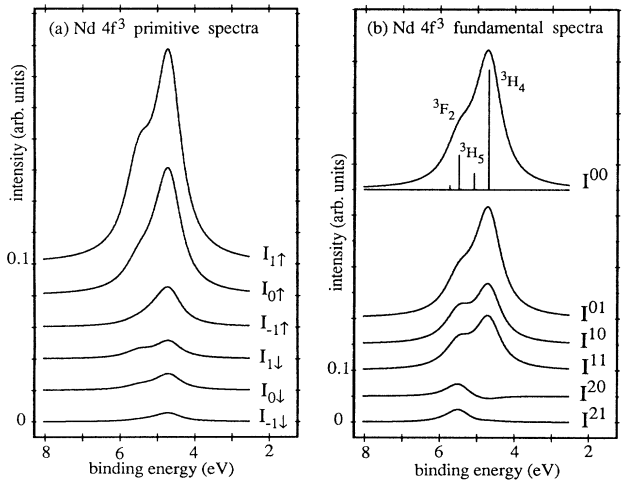

FIG. 1. (a) Primitive and (b) fundamental spectra for the photoemission Nd $4f^3 \rightarrow 4f^2\varepsilon g$ from the Hund's rule ground state $^4I_{9/2}$ with $M=-\frac{9}{2}$, calculated using Cowan's code [9] with Slater parameters $F^2=10.181$, $F^4=6.388$, $F^6=4.550$, and $\zeta_{4f}=0.119$ eV, convoluted with a Lorentzian of $\Gamma=0.37$ and a Gaussian of $\sigma=0.085$ eV [5].

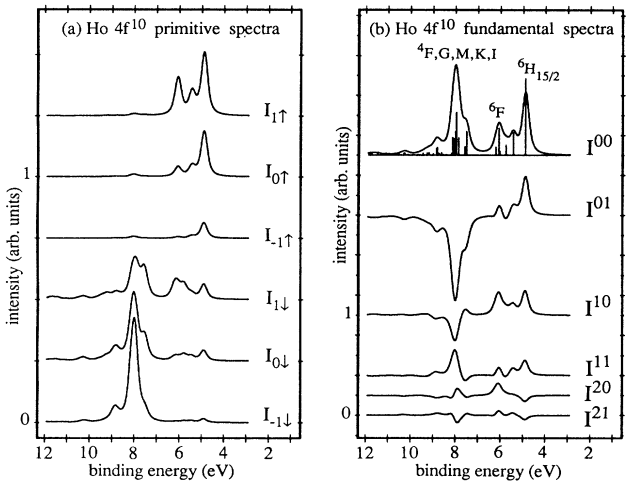

FIG. 2. (a) Primitive and (b) fundamental spectra for the photoemission Ho $4f^{10} \rightarrow 4f^9\varepsilon g$ from the Hund's rule ground state $^5I_8$ with $M=-8$, calculated using Cowan's code [9] with Slater parameters $F^2=12.567$, $F^4=7.884$, $F^6=5.598$, and $\zeta_{4f}=0.273$ eV, convoluted with a Lorentzian of $\Gamma=0.12$ and a Gaussian of $\sigma=0.085$ eV [5].

Before demonstrating the sum rules we will analyze the multiplet structure of the fundamental spectra, where each individual peak gives information about the correlation of the momenta in the corresponding final state $\underline{LSJ}$. The dependence of the spectra on $\underline{J}$ is complicated but when we sum over the $\underline{J}$ components of a term we obtain a transparent analysis in $\underline{LS}$ coupling. The spin spectrum I^{01} gives the alignment of S with the spin $\frac{1}{2}$ moment of the hole created and so the final states with low-spin ($\underline{S}=S-\frac{1}{2}$) and high-spin ($\underline{S}=S+\frac{1}{2}$) have intensities proportional to $S+1$ and $-S$, respectively, times $\langle S_z\rangle I^{00}$. For $n\leq 6$ there are only low-spin final states; therefore, the spin spectrum is proportional to the isotropic spectrum with all peaks positive [Fig. 1(b)]. For $n\geq 7$, the sign of $\langle S_z\rangle$ is reversed, and the low-spin final states have negative intensities, whereas positive intensities are obtained for the high-spin final states among which is the Hund's rule state at the low binding energy side of the spin spectrum [Fig. 2(b)].

Likewise the magnetic circular dichroism I^{10} gives the alignment of L with the orbital momentum l of the created hole when they combine to give $\underline{L}$. In LS coupling the dichroism is only determined by the orbital momenta L and $\underline{L}$ where high $\underline{L}$ values give a peak opposite to that of low $\underline{L}$ values, as is clearly seen in Ho [Fig. 2(b)]. In Nd there are only peaks with positive intensities because all $\underline{L}$ values are smaller than L [Fig. 1(b)].

The spin-orbit spectrum and magnetic circular dichroism are similar in shape for less than half-filled shells. For small spin-orbit interaction we have that $I^{11}=I^{10}(I^{01}/I^{00})$; thus with only low-spin final states the I^{11} will be proportional to the I^{10} spectrum [Fig. 1(b)]. For more than half-filled shells there are larger differences because high- and low-spin states have opposite signs and because the spin-orbit interaction increases along the $4f$ series [Fig. 2(b)]. The other fundamental spectra are more complicated and will not be discussed here. We mention that for most rare earth ions the I^{20}

TABLE I. Integrated intensities of the calculated fundamental $4f \rightarrow \varepsilon g$ spectra in Figs. 1(b) and 2(b). The ground state expectation values of the momentum products can be obtained from these integrated intensities using Eqs. (8)–(13) where $A_0=\frac{1}{7}$, $A_1=-\frac{1}{28}$, and $A_2=\frac{1}{84}$ [Eqs. (5)–(7)].

Spectrum	ρ^{xy}	Nd $4f^3$	He $4f^{10}$
Isotropic spectrum	ρ^{00}	0.42857	1.42856
Spin spectrum	ρ^{01}	0.34215	−0.54730
Magnetic circular dichroism	ρ^{10}	0.20348	0.21729
Spin-orbit spectrum	ρ^{11}	0.18139	0.20698
Linear dichroism	ρ^{20}	0.01958	0.02137
Anisotropic spin spectrum	ρ^{21}	0.02890	0.02037

and I^{21} spectra are larger than for Nd f^3 and Ho f^{10} which have small quadrupole moments.

Although the analysis of the individual structures is rather complicated, the ground state expectation values of the momentum products can simply be obtained from the integrated intensities by using the sum rules in Eqs. (8)–(13). For example, the value of $\langle S_z \rangle$ is found from ρ^{01} in Table I by using Eq. (9) with $A_0 = \frac{1}{7}$ [Eq. (5)]. Similarly, $\langle L_z \rangle$ is found from ρ^{10} by using Eq. (10) with $A_1 = -\frac{1}{28}$ [Eq. (6)]. Note that because of the spin-orbit coupling in the ground state, the values obtained are not exactly equal to those for a pure LSJ ground state, which are given by the Landé formulas

$$\langle L_z \rangle = \langle J_z \rangle \frac{J(J+1)+L(L+1)-S(S+1)}{2J(J+1)}, \qquad (14)$$

and $\langle S_z \rangle = \langle J_z \rangle - \langle L_z \rangle$. Also in the presence of crystal field interaction, hybridization, and valence mixing the value of the orbital and spin momenta can be obtained directly from polarized photoemission. This is very important for the understanding of the magnetic anisotropy in rare earth materials.

The fundamental spectra can only be measured relative to the isotropic spectrum. Consequently, the photoemission gives the expectation value of the momenta per electron, and the polarization effects are relatively larger when there are fewer f electrons. Therefore, to study the early rare earths, photoemission has an advantage over circular magnetic x-ray dichroism and resonant exchange scattering where the isotropic signal is proportional to the number of f holes [8].

In $3d$ transition metal compounds the orbital magnetic moment is 2 orders of magnitude smaller than in rare earths because of the quenching by crystal field and hybridization. This gives a proportional reduction of the circular dichroism and the effects observed in the $3d$ photoemission of Fe [10] and Co [11] are small, also because photoemission is more suited for less than half-filled shells. Larger polarization effects are expected in the actinides where the spin-orbit interaction has a magnitude comparable to that of crystal field and band structure effects.

The strong circular dichroism signal in rare earths and actinides combined with the recent availability of intense sources of polarized x rays, such as helical and crossed undulators, make it possible to study samples with a short lifetime, small size, or dilute concentration. Because the other valence electrons contribute only little to the isotropic intensity and even less to the circular dichroism, the $4f$ partial yield can be obtained by collecting all high kinetic energy electrons above a certain threshold value. The electrons emitted from closed shells do not give a net effect, but discrimination of these low kinetic energy electrons reduces the background. This partial-yield detection can be applied in photoelectron microscopy to measure the spatial resolution of the magnetic domain structure of ferromagnetic and ferrimagnetic materials. The magnitude of the circular dichroism signal for each domain is determined by the relative orientation of its orbital magnetic moment and the direction of the incident x-ray beam.

In conclusion, we can say that by introducing some simple techniques we are able to obtain a deeper understanding of which properties are measured using light and spin polarization in open shell photoemission. This is very important for the planning and the analysis of the growing number of experimental possibilities to study the magnetic properties of rare earths. The strong polarization effects combined with the surface sensitivity of photoemission offer unique possibilities, such as photoelectron microscopy, to characterize surfaces and thin films.

[1] See, e.g., P. Carra and M. Altarelli, Phys. Rev. Lett. **64**, 1286 (1990); C. T. Chen, F. Sette, Y. Ma, and S. Modesti, Phys. Rev. B **42**, 7262 (1990); Y. Wu, J. Stöhr, B. D. Hermsmeier, M. G. Samant, and D. Weller, Phys. Rev. Lett. **69**, 2307 (1992).

[2] B. T. Thole and G. van der Laan, Phys. Rev. B **44**, 12424 (1991).

[3] L. Baumgarten, C. M. Schneider, H. Petersen, F. Schäfers, and J. Kirschner, Phys. Rev. Lett. **65**, 492 (1990).

[4] M. Campagna, G. K. Wertheim, and Y. Baer, in *Photoemission in Solids II,* edited by L. Ley and M. Cardona (Springer-Verlag, Berlin, 1979).

[5] J. K. Lang, Y. Baer, and P. A. Cox, J. Phys. F **11**, 121 (1981).

[6] F. Gerken, J. Phys. F **13**, 703 (1983).

[7] K. Starke, E. Navas, L. Baumgarten, and G. Kaindl (to be published).

[8] B. T. Thole, P. Carra, F. Sette, and G. van der Laan, Phys. Rev. Lett. **68**, 1943 (1992).

[9] R. D. Cowan, *The Theory of Atomic Structure and Spectra* (University of California Press, Berkeley, 1981).

[10] C. M. Schneider, M. S. Hammond, P. Schuster, A. Cebollada, R. Miranda, and J. Kirschner, Phys. Rev. B **44**, 12066 (1991).

[11] J. Bansmann, C. Westphal, M. Getzlaff, F. Fegel, and G. Schönhense, J. Magn. Magn. Mater. **104–107**, 1691 (1992).